PHYSICAL REVIEW C VOLUME 25, NUMBER 1 JANUARY 1982

High spin states of ^{84}Sr

A. Dewald, U. Kaup, W. Gast, A. Gelberg, H.-W. Schuh, K. O. Zell, and P. von Brentano
Institut für Kernphysik der Universität zu Köln, D-5000 Köln 41, West Germany
(Received 26 June 1981)

^{84}Sr has been investigated by means of conventional in-beam gamma-ray spectroscopy with the reactions ^{76}Ge(^{12}C,4n) and ^{81}Br(^{6}Li,3n). Lifetimes of 10 levels have been measured by the recoil distance Doppler shift technique. Four positive and at least two negative parity bands have been found. The energies of the ground state band and quasigamma band as well as the $E2$ transition strengths are compared with theoretical values obtained from the proton-neutron interacting boson model. A relatively long lived 8^+ state has been found, to which we assign the $(\nu g_{9/2})^{-2}$ configuration.

NUCLEAR REACTIONS ^{76}Ge(^{12}C,4$n\gamma$), $E=48-60$ MeV; ^{81}Br(^{6}Li,3$n\gamma$), $E=19-32$ MeV, measured E_γ, I_γ, $\gamma\gamma$ coincidence, γ angular distribution, recoil distance Doppler shift; ^{84}Sr deduced levels, J, π, τ. Enriched targets, Ge(Li) detectors.

I. INTRODUCTION

The ground state bands of Sr isotopes with $A \leq 88$ show a gradual transition from the nearly doubly magic nucleus ^{88}Sr to the rotational-like ^{80}Sr. The fact that the proton number $Z=38$ or 40 can be considered magic, at least when the neutron number is 50, makes the investigation of this transition quite interesting.

Shell model calculations have been carried out in the mass $A=90$ region by Talmi and Unna[1] and Auerbach and Talmi.[2] Kitching[3] and Ogawa[4] have described low lying excitations in the lighter Sr isotopes as two-hole states. They obtained good agreement with the experiment especially for ^{86}Sr by considering the excited states to belong mainly to the configuration $(\nu g_{9/2})^{-2}$ The description of the isotopes ^{84,82,80}Sr was less successful. Ogawa succeeded only in getting their gross features by introducing additional two-proton-hole excitations. The question arises as to how far from ^{88}Sr one can still find low-lying quasiparticle excitations.

^{84}Sr, which is four neutron holes away from ^{88}Sr, should display both collective and quasiparticle excitations; this makes it an interesting object of investigation.

Low spin states of ^{84}Sr have already been studied by β decay,[5] as well as by (p,t) (Refs. 6 and 7) and (α,α') (Ref. 8) reactions. Measurements using the reactions ^{76}Ge(^{12}C,4n) (Ref. 9) and ^{85}Rb(p,2n) (Ref. 10) have also been performed, the latter being suitable to the population of the quasigamma band. The aim of the present work was to investigate the high spin states and the side bands by means of in-beam gamma-ray spectroscopy, and to try to group the states into bands according to their decay properties.

II. EXPERIMENTAL METHODS AND RESULTS

A list of experiments, reactions, and targets is given in Table I. All measurements were carried out at the FN tandem Van de Graaff accelerator in Cologne. The gamma rays were measured by means of Ge(Li) detectors with energy resolutions of 1.8–2.1 keV at 1408 keV and 0.7–1.2 keV at 244 keV, and with relative efficiencies of 11–17%. The data were accumulated in a PDP-11/20 computer system used either as a 2×8192 or a 4×4096 multichannel analyzer. A singles spectrum of the reaction ^{81}Br(^{6}Li,3n)^{84}Sr taken at 55° with respect to the beam direction is given in Fig. 1.

$\gamma\gamma$ coincidences were measured by means of a standard three parameter coincidence system with a time resolution of about 10 ns in the energy range 0.1–2 MeV. Two large volume Ge(Li) detectors were positioned either at 90°–270° or at 0°–90°. The singles counting rate was about 10 kHz for each detector corresponding to a coincidence counting rate of about 1.5 kHz. The coin-

 ©1982 The American Physical Society

TABLE I. List of experiments, reactions, and targets.

Measurement	Reaction	Beam energy (MeV)	Element (compound)	Enrichment (%)	Thickness (mg/cm^2)	Goldbacking thickness (mg/cm^2)
$\gamma\gamma$ coincidence	(^{6}Li,3n)	28	Tl^{81}Br	97.8	3.8	
$\gamma\gamma$ coincidence	(^{12}C,4n)	60	^{76}Ge	92.8	1	4
$\gamma\gamma$ coincidence	(^{12}C,4n)	58.3	^{76}Ge	92.8	1	4
γ-excitation function	(^{6}Li,3n)	25, 26, 28, 30, 32	Tl ^{81}Br	97.8	1.8	
γ-excitation function	(^{6}Li,3n)	19, 21, 23, 25, 27, 28, 30	Tl ^{81}Br	97.8	2	0.1 + 1[a]
γ-excitation function	(^{12}C,4n)	48, 51, 54, 56, 58, 60	^{76}Ge	95.5	4	1+4[a]
γ-angular distribution	(^{6}Li,3n)	28	Tl ^{81}Br	97.8	3.5	0.1 + 1[a]
γ-angular distribution	(^{12}C,4n)	60	^{76}Ge	92.8	1	0.1
RDDS	(^{12}C,4n)	60	^{76}Ge	92.8	0.6	1

[a]Sandwich.

cidence events were recorded on magnetic tape. All events lying in a 43 ns time window on the prompt peak were sorted off line into an $8k \times 8k$ disc stored matrix on which the energy windows were set later on. The subtraction of the coincidence background was done in the conventional way.

Coincidence data obtained from the reactions ^{81}Br(^{6}Li,3n)^{84}Sr and ^{76}Ge(^{12}C,4n)^{84}Sr are given in Table II. A few coincidence spectra from the reaction ^{81}Br(^{6}Li,3n)^{84}Sr are shown in Fig. 2.

In order to measure excitation functions, two detectors were positioned at 55° and 125° for the ^{12}C and at 90° and 270° for the ^{6}Li induced reaction; the detector to target distance was about 15 cm. The spectra were normalized to the integrated beam charge. Figure 3 shows examples of relative excitation functions for the ^{12}C induced reaction.

Angular distributions were measured at six angles with the detectors at about 15 cm from the target. Some strong and well resolved ^{84}Sr lines detected by a fixed Ge(Li) were used to normalize the spectra; a pulser triggered by the beam was used to compensate dead time effects.

The A_2 and A_4 coefficients obtained by fitting the usual Legendre polynomial expansion to the experimental data are given in Table III.

A χ^2 analysis was performed, assuming a Gaussian distribution of the magnetic substates. The free parameters are the mixing ratios and the widths of the magnetic quantum number distribution. Figure 4 shows the angular distributions of some lines and Fig. 5 a few χ^2 curves for the 1001 keV transition.

Lifetimes of excited states populated in the ^{76}Ge(^{12}C,4n)^{84}Sr reaction were measured by the recoil distance Doppler shift technique (RDDS). A 0.6 mg/cm^2 ^{76}Ge target evaporated on a 1.6 mg/cm^2 Au foil and a 10 μm Ta stopper foil were mounted in a plunger system.[11] The beam was completely stopped in an additional 20 μm Ta foil. The flight distance was varied in a 0−6000 μm range by changing the target position with a micrometer screw.

The distance could be directly read out in the 0−200 μm range by a magnetic transducer with an accuracy of about 1%. The capacity between target and stopper was measured by means of a pulser[12] during the whole experiment, and was used as a stability check of the distance. Keeping the ^{12}C beam on for the whole duration of the experiment, it was found that the thermal drifts of the plunger system were less than 0.2 μm during a

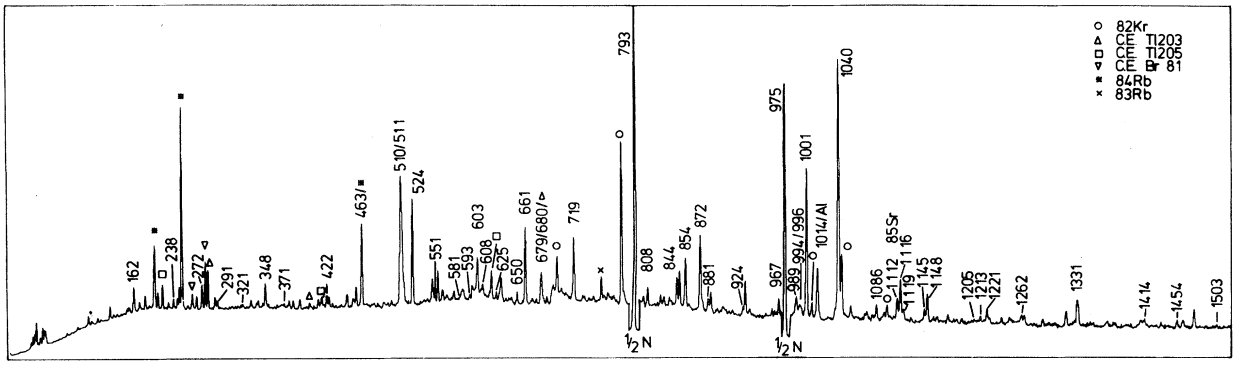

FIG. 1. Gamma-ray singles spectrum of ^{81}Br(^{6}Li,3n)^{84}Sr at 28 MeV taken at 55° relative to the beam axis. The counting rate per channel is multiplied by the channel number as a rough correction for the detector efficiency. The energies are given in keV.

normal one hour run. Three Ge(Li) detectors were positioned at 160°, 55°, and 0° at about 15 cm distance from the target. The recoil velocity estimated from the Doppler shift was

$$\frac{v}{c}=0.0125\pm0.0005 .$$

The intensities of the shifted and unshifted peaks were determined by a procedure different from the conventional one.

Spectra taken at different distances were normalized to the 301 keV Coulomb excitation line from the Ta stopper. Each normalized spectrum was subtracted from the spectrum taken at a target-stopper distance so long that all the unshifted peaks of interest vanish. Thus one gets a negative unshifted peak and a positive shifted peak. The positive and the negative peaks have the same area which is equal to the area of the unshifted peak in the usual spectrum. Therefore the areas of unshifted peaks in the difference spectrum could be used in the lifetime estimation. In the same way one could obtain the area of the shifted peaks by subtracting each spectrum from the spectrum taken at zero distance between target and stopper.

The method described above considerably simplifies the analysis of the data; one important feature of the subtracted spectra is the flatness of the background within a wide energy interval. The procedure is also able to detect contaminating lines by means of careful investigation of the positive and the corresponding negative peak. Figure 6 compares a typical difference spectrum with a standard one.

The areas of corresponding positive and negative peaks in the difference spectra are equal only as long as deorientation effects by the hyperfine field and solid angle corrections are not considered. The effect of deorientation was neglected for reasons described by Rascher *et al.*[13] As the stopper was fixed during the measurement, no solid angle correction was needed for the unshifted peak. The effect of the solid angle on the area of the shifted peak was found to be negligible for target-stopper distances below 4000 μm.

The decay functions obtained were analyzed by using the program CRONOS (Ref. 14) which can handle delayed feedings from six different levels in any arrangement. The continuum feeding with typical times of about 0.1 ps in this mass region[15] was neglected. The intensities used in this analysis were taken from the angular distribution measurement, and were checked in an experiment under the same conditions as in the plunger one, with detectors positioned at 55° and 125°.

The measured lifetimes and $B(E2)$ values are given in Table IV. Figure 7 displays a few decay curves of lines belonging to the ground state band.

The level scheme inferred from the coincidence measurements is shown in Fig. 8. Spin and parity assignments are based on angular distribution and excitation function data.

The level scheme is in reasonable agreement with those given previously.[5,6,10] The main discrepancy concerns the energies of the 8^+ and 10^+ states of the yrast cascade. Our coincidence measurements indicate that there is a 524 keV gamma transition located between the 1116 and 1040 keV lines, which has not been observed by Inamura *et al.*[9] Moreover, the decay curves of all transitions located below the 3332 keV 8^+ state show a component with $\tau=226$ ps (Fig. 7), which is not displayed by the 1116 keV transition.

Twenty-two levels and 37 gamma transitions

TABLE II. Coincidence results from the reactions ^{76}Ge(^{12}C,4n)^{84}Sr and ^{81}Br(^{6}Li,3n)^{84}Sr. The areas of the peaks in the coincidence spectra are given in parentheses. The estimated error of the background area under a peak is given in brackets after the gate energy.

Reaction ^{81}Br(^{6}Li,3n)^{84}Sr Gate (keV)	Coincident γ rays (keV)
162[30]	162(72), 179[a](49), 254[a](59), 416[a](60), 719(98), 793(174), 975(85), 1001(96);
238[40]	272(199), 371(58), 593(64), 793(185), 1001(139);
272[40]	238(243), 609(96), 793(487), 975(485), 1001(320);
291[40]	276[a](102), 650(60), 793(178), 975(145), 1040(107);
321[30]	510(77), 793(130);
348[40]	524(365), 793(314), 854(120), 975(359), 1040(336), 1119(80);
371[40]	238(57), 510(249), 975(100), 1001(116);
422[40]	603(204), 661(123), 679(193), 793(352), 968(242), 975(242), 1213(82);
463[40]	793(287), 975(180), 1040(210);
510[60]	321(83), 371(253), 511[e](3043), 584[c](150), 743[a](147), 761[c](229), 777[f](135), 793(927), 974(672), 989(245), 1001(1318), 1041[a](183), 1377[a](133);
524[50]	348(395), 793(1625), 975(1424), 1014[a](83), 1040(1343), 1116(411), 1414(100);
552[40]	793(184), 975(161), 1331(68);
581[40]	793(80), 975(80), 1040(80);
593[40]	238(70), 661(50), 793[c](181), 974[c](80), 994(60), 1040[c](80);
603[40]	422(141), 661(670), 679(163), 1040[c](107);
609[50]	272(100);
625[40]	793(138), 1001(95);
650[40]	793(100), 975(100), 1331(88);
661[40]	422(90), 510(100), 603(664), 679(207), 686[a](88), 793(1160), 844(78), 994(192), 1145(111);
680[40]	422(142), 603(162), 661(167), 793(653), 975(399), 1040(242), 1112[g](93), 1148(78) 1289[g](82);
719[40]	162(153), 321(77), 358[a](61), 793(692), 808(160), 975(664), 1001(621), 1148(181);
780[30]	719(30), 975[c](160), 1001(100), 1040[c](90);
793[60]	162(149), 205[a](120), 209[a](150), 238(219), 272(551), 321(60), 348(385), 422(342), 443[a](108), 463[b](179), 510(877), 524(1778), 552(179), 603(619), 625(190), 650(100), 661(1249), 680(586), 719(685), 808(170), 844(212), 854(531), 872(896), 924[a](141), 967(232), 975(6485), 989(180), 993(213), 1001(1962), 1015[a](256), 1040(2884), 1086(178), 1116(264), 1119(130), 1145(90), 1148(209), 1221(200), 1263(181), 1331(253), 1414(116), 1503(95);
808[40]	625(84), 719(119), 793(238), 994(152), 1001(104), 1148(89);

TABLE II. *(Continued.)*

Reaction ^{81}Br(^{6}Li,3n)^{84}Sr	
Gate (keV)	Coincident γ rays (keV)
844[40]	661(106), 793(80), 975[c](80);
854[40]	348(127), 524(70), 581(72), 793(555), 872(433), 975(526), 1040(333), 1119(130);
872[40]	793(876), 854(384), 975(783), 1040(808), 1119(100);
881[30]	321(37), 516[a](65), 793(60), 803[a](86), 975(50), 1001(70);
924[a][30]	793(130), 975(130), 1040(100);
968[30]	422(212), 793(166), 975(168);
975[70]	162(134), 225[a](100), 238(138), 244[a](88), 272(382), 291(120), 348(348), 371(123), 422(152), 463[b](143), 510(707), 524(1345), 552(114), 625(129), 650(146), 680(272), 719(602), 793(6556), 808(120), 854(412), 872(713), 968(279), 989(192), 1001(1476), 1015[a](201) 1040(2382), 1086(97), 1116(202), 1119(100), 1148(159) 1331(183), 1503(99);
989[30]	510(198), 975(181), 1001(115);
994[50]	661(304), 793(140);
997	
1001[50]	162(88), 238(141), 272(346), 348(86), 371(125), 510(1038), 625(142), 719(652), 760[a](118), 793(1718), 808(88), 860[a](76), 881(89), 975(1500), 989(185), 1015[a](89), 1075[a](100), 1086(114), 1148(108);
1015[a][30]	258[a](50), 552(63), 793(178), 975(100), 1040(100);
1040[40]	253[a](70), 291(150), 348(153), 463[b](112), 510(123), 524(1428), 603[c](136), 661[d](149), 680(196), 793(3118), 854(399), 872(763), 924[a](95), 974(2460), 1015[a](96), 1116(340), 1221(110);
1075[a][40]	777[f](99), 793(159), 975(110), 1001(130);
1086[30]	793(161), 975(162), 1040(80);
1116[30]	524(516), 793(438), 975(376), 1040(320);
1119[30]	348(60), 524(87), 793(234), 854(80), 872(85), 975(128), 1040(106);
1145[30]	661(171), 793(184), 975[d](120);
1148[40]	625(63), 680(100), 719(165), 793(267), 808(148), 975(258), 1001(183), 1040(90);
1206	
1213[30]	422(74), 679(56);
1221[30]	793(193), 975(120), 1040(136);
1263[30]	793(121);
1331[30]	552(88), 793(262), 994(167), 1086(53);
1414[30]	524(65), 793(136), 975(130), 1040(75);

TABLE II. *(Continued.)*

Reaction ^{81}Br(^{6}Li,3n)^{84}Sr	
Gate (keV)	Coincident γ rays (keV)
1454[20]	603(66);
1503	

Reaction ^{76}Ge(^{12}C, 4n)^{84}Sr	
Gate (keV)	Coincident γ rays (keV)
348[30]	524(90), 793(100), 854(50), 975(60), 1040(70), 1119(50);
415[a][30]	510(60), 625(94), 707[a](60), 793(86), 975(60), 1001(74), 1201[a](52);
432[a][30]	415[a](60), 707(61), 793(70), 808(50), 1001(50);
510[40]	415[a](63), 511(3183), 617[h](62), 689(58), 793(127), 975(136), 989(59), 994(62), 1001(195);
524[40]	348(101), 793(314), 854(80), 975(318), 997(60), 1040(361), 1116(169), 1206(60), 1414(90);
625[35]	415[a](95), 719(60), 793(50), 808(70), 975(60), 1001(50);
680[30]	793(98), 975(70), 1040(70);
707[a][30]	415[a](60), 432[a](74), 793(100), 975(50);
719[40]	625(78), 793(163), 808(60), 975(93), 1001(124), 1148(90);
793[30]	348(53), 415[a](72), 510(98), 524(373), 625(88), 708[a](97), 719(193), 808(106), 854(260), 872(257), 974(936), 1001(268), 1040(579), 1086(121), 1116(99), 1119(60), 1148(80), 1451[d](67), 1501[a](62);
808[30]	625(70), 719(75), 793(103), 1001(75), 1148(78);
854[30]	348(50), 524(78), 793(248), 872(167), 975(302), 1040(173), 1086(80), 1119(105);
872[30]	793(214), 854(223), 975(282), 1040(200), 1086(60), 1119(85);
975[40]	348(69), 415[a](69), 510(103), 524(430), 707[a](50), 719(110), 793(1029), 808(144), 854(199), 872(162), 1001(210), 1040(590), 1086(85), 1116(94), 1119(60), 1148(106);
989[30]	510(70), 1001(60);
997[30]	625(47), 793(50), 1116(50);
1001[40]	415[a](74), 510(215), 625(72), 719(156), 793(201), 808(60), 975(190), 989(62), 1148(74);
1040[40]	348(70), 415[a](70), 510(70), 524(425), 680(70), 793(692), 854(252), 872(256), 975(626), 1086(76) 1116(105), 1119(70);
1086[30]	348(54), 524(60), 793(138), 854(69), 872(69), 975(107), 1040(74), 1119(60);
1116[25]	524(191), 793(185), 975(175), 1040(100), 1206(51);
1119[25]	348(44), 793(153), 854(106), 872(77), 975(121), 1040(100), 1086(60);
1148[30]	625(40), 680(40), 719(78), 793(120), 808(76), 974(84), 1001(60);
1201[a]	

TABLE II. *(Continued.)*

Reaction ^{76}Ge(^{12}C, 4n)^{84}Sr	
Gate (keV)	Coincident γ rays (keV)
1205[30]	524(67), 793(70), 975(70), 1040(50), 1116(50),
1414[30]	793(72);

[a]Not assigned.
[b]^{84}Rb.
[c]Compton backscattering.
[d]Conflicting assignment.
[e]$e^+ - e^-$ annihilation.
[f]^{82}Kr.
[g]^{85}Sr.
[h]^{80}Kr.

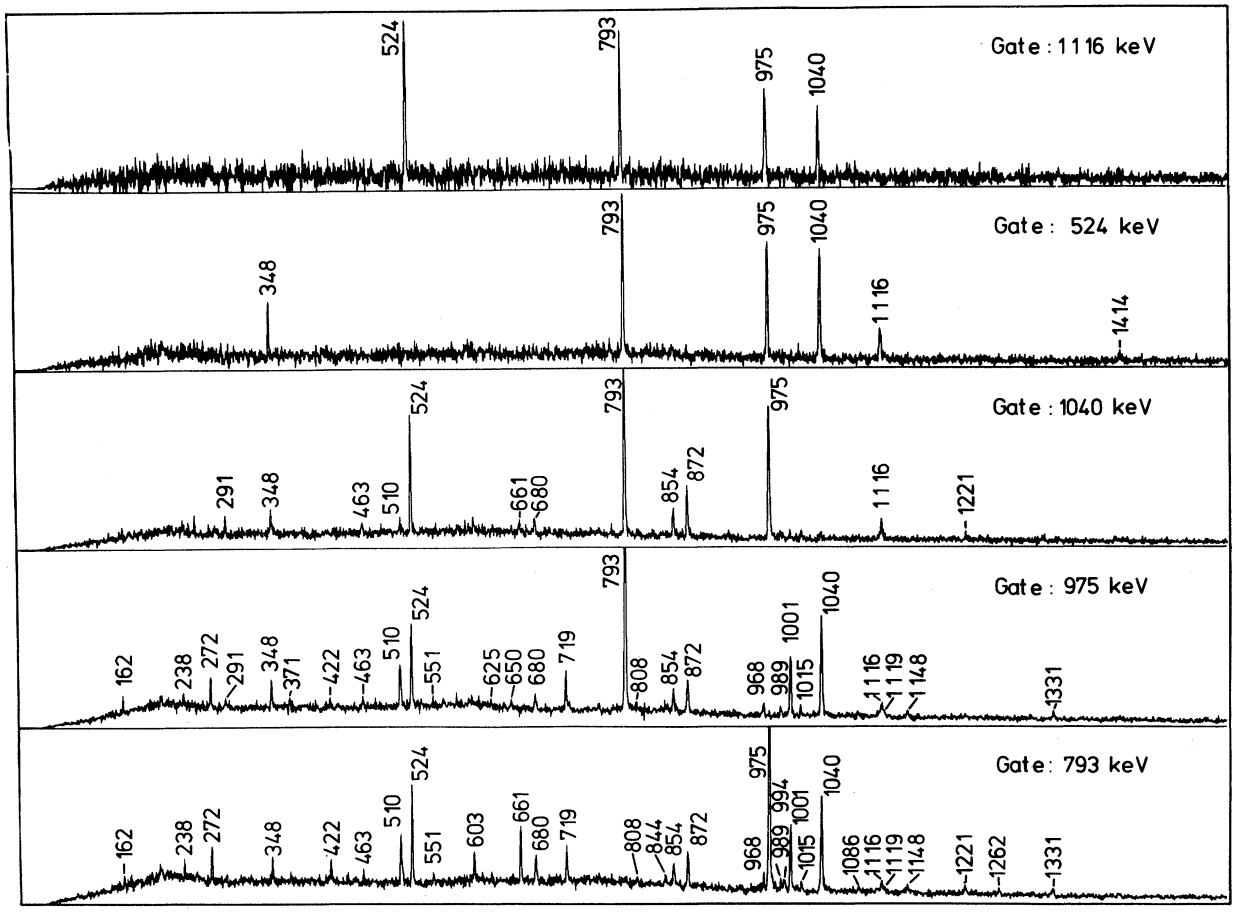

FIG. 2. A few coincidence spectra with gates on the lowest five members of the yrast cascade found in the ^{81}Br(^{6}Li,3n)^{84}Sr reaction.

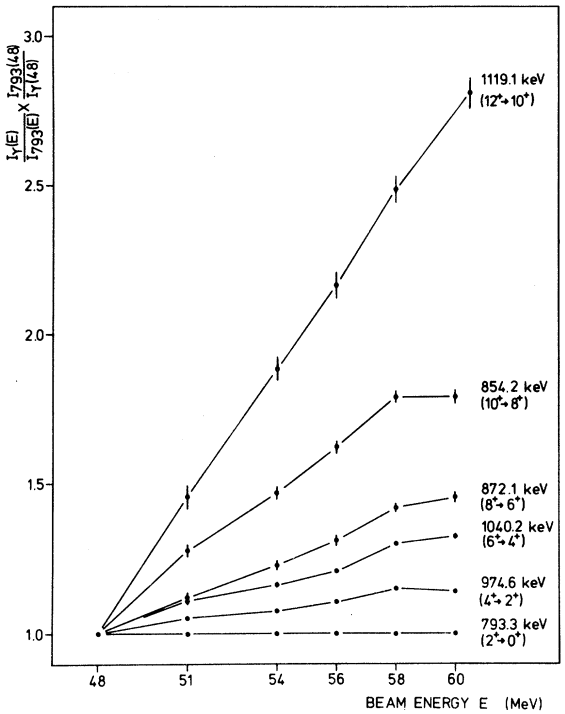

FIG. 3. Excitation functions of some gamma-ray transitions observed via the reaction ^{76}Ge(^{12}C,4n)^{84}Sr.

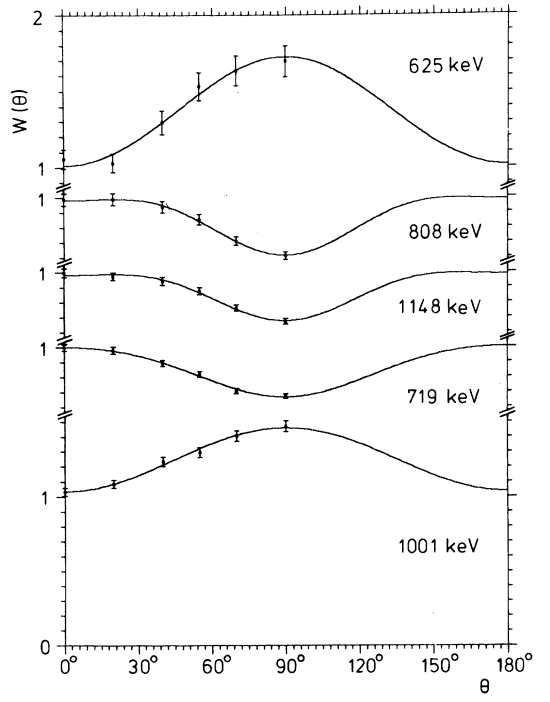

FIG. 4. Experimental angular distributions of transitions of the negative parity band obtained in the reaction ^{76}Ge(^{12}C,4n)^{84}Sr. The experimental data were fitted with the Legrendre polynomial expansion $\omega(\theta)=A_0+A_2P_2[\cos(\theta)]+A_4P_4$ [cos (θ)].

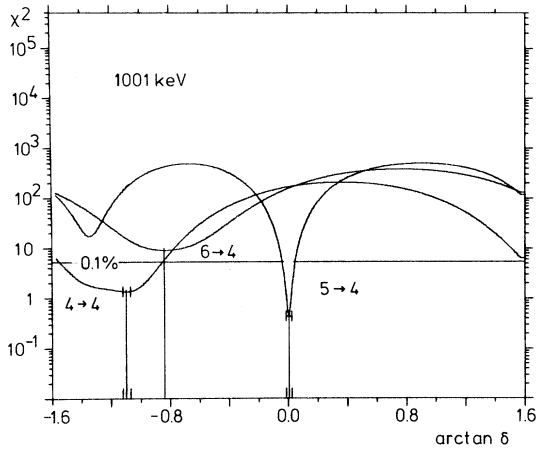

FIG. 5. χ^2 versus arctan(δ) plot for some spin hypotheses of the 1001 keV transition.

were added to those already known. The yrast cascade has been extended up to $I^\pi=14^+$. Negative parity states have been identified up to 11^-. The presence of two 5^- and 7^- states indicates that there is more than one negative parity band. Spin and parity assignments for the negative parity bands are based on the 3^- assignment for the 2448 keV and 5^- for the 2769 keV levels. The spin-parity assignment of the 2448 keV level was given by Ball *et al.*[6] We deduced spin 5 for the 2769 keV level from angular distributions and excitation functions. Yoshikawa *et al.*[10] assigned a negative parity to this state which is in agreement with the mixing ratio $\delta=0$ we found from the angular distribution of the 1001 keV transition as expected for $E1$. In addition the 321 keV branching to the 3^- state excludes $M1$ or $E2$ for the 1001 keV transition and confirms the parity assignment for the 2769 keV level. Some less definite spin-parity assignments will be now discussed in more detail.

A. 4029 and 2599 keV levels

The angular distribution functions of the 1221 and 1145 keV transitions indicate either $\Delta I=0$ or $\Delta I=2$. Therefore the assignments 6^+ or 8^+ for the 4029 keV state and 2^+ or 4^+ for the 2599 keV state are possible. We favor 8^+ for the 4029 keV level and 4^+ for the 2599 level on the basis of excitation functions.

TABLE III. Energies, relative intensities, and angular distribution coefficients of γ rays observed in the reaction ^{81}Br(^{6}Li,3n)^{84}Sr at 28 MeV.

E_γ (keV)	I_γ^{rel}	A_2/A_0	A_4/A_0	$I_i \rightarrow I_f$
162.2(2)	21(1)	0.41(1)	0.00(1)	$7^- \rightarrow 7^-$
237.9(1)	11(1)	−0.25(4)	0.09(8)	$6^- \rightarrow 5^-$
272.2(1)	30(1)	0.25(6)	0.00(1)	$5^- \rightarrow 5^-$
290.8(1)	13(1)	0.23(27)	0.00(1)	$6^+ \rightarrow 6^+$
321.0(1)	6(1)			$5^- \rightarrow 3^-$
348.0[a](1)	33(1)	−0.36(6)	−0.06(3)	$8^+ \rightarrow 8^+$
371.0(1)	5(1)	−0.53(24)	0.01(2)	$7^+ \rightarrow 6^-$
421.8(1)	28(1)	0.27(5)	−0.08(4)	$(7^+) \rightarrow (5^+)$
462.7[b](2)	10(1)			
510.1[b](5)	64(1)			$6^- \rightarrow 5^-$
524.1(1)	136(3)	0.32(2)	−0.07(1)	$8^+ \rightarrow 6^+$
551.5(2)	9(1)	−0.36(7)	0.04(1)	$7^- \rightarrow 6^+$
581.3(2)	5(1)			$8^+ \rightarrow 6^+$
593.3(2)	8(1)			$5^- \rightarrow 3^-$
602.5(1)	71(3)	0.18(3)	0.05(1)	$3^+ \rightarrow 2^+$
608.9(1)	23(1)			$7^- \rightarrow 5^-$
625.1[a](2)	11(1)	−0.33(5)	0.01(6)	$(12) \rightarrow 11^-$
650.4(2)	13(1)	−0.44(5)	0.16(4)	$7^+ \rightarrow 6^+$
660.9(1)	106(3)	0.14(3)	0.00(1)	$2^+ \rightarrow 2^+$
679.1[b](2)	26(3)			$(5^+) \rightarrow 3^+$
680.1[a,b](2)	39(4)	−0.31(4)	0.16(5)	$7^- \rightarrow 6^+$
718.9(1)	90(5)	0.31(3)	−0.05(1)	$7^- \rightarrow 5^-$
780.1(2)	13(1)			$8^- \rightarrow 7^-$
793.3(1)	1000(46)	0.23(1)	−0.05(1)	$2^+ \rightarrow 0^+$
808.4(1)	23(2)	0.38(8)	−0.19(8)	$11^- \rightarrow 9^-$
844.0(1)	51(2)			
854.2(1)	77(2)	0.30(3)	−0.05(1)	$10^+ \rightarrow 8^+$
872.1(1)	113(3)	0.33(3)	−0.05(1)	$8^+ \rightarrow 6^+$
881.1(2)	12(1)	0.12(2)	−0.10(6)	$7^- \rightarrow 5^-$
967.9(1)	22(1)	0.38(7)	0.07(2)	$(5^+) \rightarrow 4^+$
974.6(1)	773(39)	0.30(1)	−0.07(1)	$4^+ \rightarrow 2^+$
988.9(1)	27(1)	0.30(7)	−0.13(5)	$8^- \rightarrow 6^-$
994.0(3)	16(1)	−0.25(5)	0.005(3)	$3^- \rightarrow 2^+$
996.9(3)	7(1)			$11^- \rightarrow 10^+$
1001.4(1)	217(19)	−0.18(1)	0.012(1)	$5^- \rightarrow 4^+$
1040.2(1)	426(9)	0.27(2)	−0.06(1)	$6^+ \rightarrow 4^+$
1086.4[a](1)	26(2)	0.16(3)	−0.06(1)	$14^+ \rightarrow 12^+$
1115.7(1)	67(3)	0.27(4)	−0.09(2)	$10^+ \rightarrow 8^+$
1119.1[a](1)	24(1)	0.33(2)	−0.14(2)	$12^+ \rightarrow 10^+$
1144.5(2)	15(2)	0.15(13)	−0.05(5)	$(4^+) \rightarrow 2^+$
1148.2(1)	41(2)	0.30(6)	−0.08(4)	$9^- \rightarrow 7^-$
1205.6[a](2)	8(1)	0.26(6)	−0.03(2)	$12^+ \rightarrow 10^+$
1213.3(2)	10(1)	0.33(7)	0.09(10)	$(9^+) \rightarrow (7^+)$
1220.9(2)	16(8)	0.20(9)	−0.16(6)	$(8^+) \rightarrow 6^+$
1263.4(5)	8(1)	−0.47(28)	0.09(11)	$3^+ \rightarrow 2^+$
1331.0(2)	35(2)	0.36(1)	−0.06(1)	$6^+ \rightarrow 4^+$
1413.8(2)	11(1)			
1454.2(2)	14(1)			$2^+ \rightarrow 0^+$
1502.9(3)	3(1)			

[a]The angular distribution coefficients of the line were obtained from the analysis of the ^{76}Ge(^{12}C,4n)^{84}Sr reaction data.
[b]Doublets; the intensities are approximate estimates.

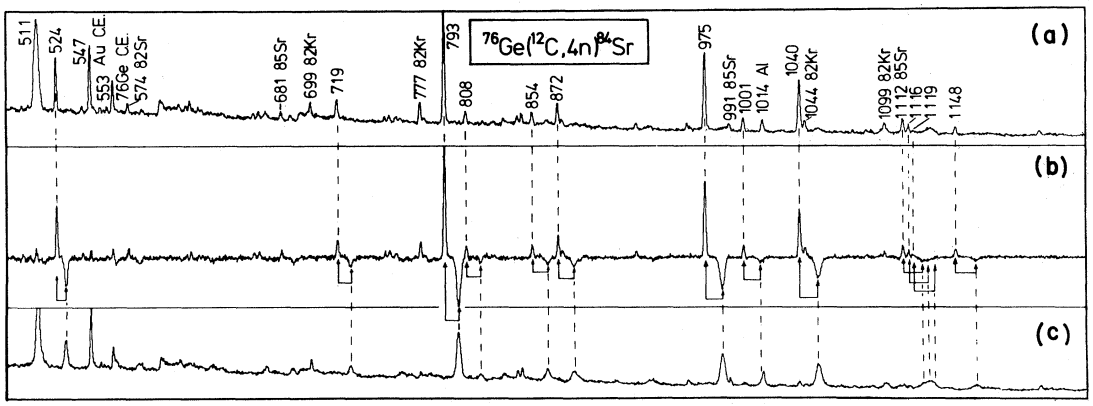

FIG. 6. (a) Conventional spectrum from the plunger experiment at contact between target and stopper; (c) same, at 6000 μm; Spectrum (b) is the difference of the normalized spectra (a) and (c).

B. 2736 keV level

The 2736 keV level is depopulated by a 968 and a 679 keV transition, respectively, to the 1768 and 2057 keV levels. The 679 keV line is a doublet, so only the angular distribution of the 968 keV peak could be analyzed. It was found to be a $\Delta I=1$ transition. Its excitation function is compatible with spin 5 for the 2736 keV level. A comparison with neighboring nuclei confirms the spin 5 assignment. The 679 keV branching to the 2057 keV 3^+ state indicates positive parity for the 2736 keV level. Due to the weak intensity of the 968 keV line the spin assignment is not definite.

C. 3158 keV level

The 3158 keV level is deexcited by a 422 keV γ ray to the 2736 keV level. The 422 keV transition was found to have either $\Delta I=0$ or $\Delta I=2$. The assignment (7^+) was made as the excitation function of that γ ray indicates spin 7.

D. 4371 keV level

The level decays via a 1213 keV γ ray to the 3158 keV state. The angular distribution suggests $\Delta I=0$ or $\Delta I=2$, but $\Delta I=1$ is also possible. Due

TABLE IV. Lifetimes and $B(E2)$ values measured in the reaction ^{76}Ge(^{12}C,4n)^{84}Sr using the RDDS technique.

State E_x (keV)	I^π	τ (ps)	Transition E_γ (keV)	$I_i \rightarrow I_f$	$B(E2)$ (e^2fm^4)	$B(E2)$ W.u.[a]
793	2^+	4.6(5)	793	$2^+ \rightarrow 0^+$	570(60)	26(3)
1768	4^+	2.5(3)	975	$4^+ \rightarrow 2^+$	370(50)	17(2)
2769	5^-	13.7(8)	1001	$5^- \rightarrow 4^+$		
2769	5^-	13.7(8)	321	$5^- \rightarrow 3^-$	460(60)	21(3)
2808	6^+	1.5(3)	1040	$6^+ \rightarrow 4^+$	450(90)	21(4)
3332	8^+	226(7)	524	$8^+ \rightarrow 6^+$	92 (3)	4.2(2)
3488	7^-	6.3(7)	719	$7^- \rightarrow 5^-$	490(60)	22(3)
3680	8^+	4.8(2)	872	$8^+ \rightarrow 6^+$	270(10)	12(1)
4448	10^+	3.2(5)	1116	$10^+ \rightarrow 8^+$	150(20)	7(1)
4534	10^+	2.4(2)	854	$10^+ \rightarrow 8^+$	750(60)	34(3)
4636	9^-	3.6(6)	1148	$9^- \rightarrow 7^-$	110(20)	5(1)
5445	11^-	10.8(14)	808	$11^- \rightarrow 9^-$	220(30)	10(1)
5654	12^+	1.2(4)	1119	$12^+ \rightarrow 10^+$	310(100)	14(5)
5654	12^+	1.2(4)	1205	$12^+ \rightarrow 10^+$	62(20)	(3(1)

[a]Weisskopf units.

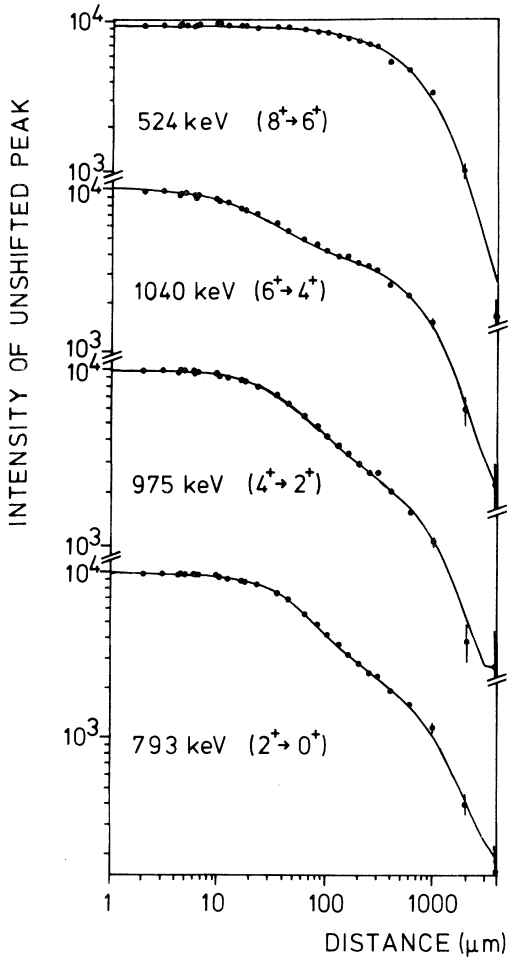

FIG. 7. Decay curves of the lowest members of the yrast cascade.

to the excitation function of this line we prefer the assignment $J^{\pi}=9^{+}$.

III. DISCUSSION

The levels of ^{84}Sr can be grouped into bands by using the $B(E2)$ values. Such a tentative classification is shown in Fig. 9.

The ground state band (gsb), whose transitions are characterized by rather large collective $B(E2)$'s can be followed up to the 2808 keV 6^{+} state. The 8^{+}, 3332 keV state decaying by the 524 keV transition with a $B(E2)$ of 4.2 Weisskopf units (W.u.) does not belong to this band. We will return to this point later on. The weakly populated 4029 keV state, whose spin assignment (6^{+} or 8^{+}) is ambiguous, is apparently the 8^{+} level of the gsb. Its energy corresponds to what we could expect by extrapolating the gsb energies; moreover it decays only to the gsb 6^{+} state.

We consider the second 2^{+} and the 3^{+} states members of the quasigamma band as already done by Yoshikawa *et al.*[10] The similarity to neighboring nuclei suggests that the 2736 keV 5^{+} state and probably the 2298 keV level for which we do not have a reliable spin assignment also belong to this band. Encouraged by the collective aspect of the gsb, we tried to describe its states and the members of the quasigamma band by means of the proton-neutron interacting boson model[16] (IBM).

Calculations for the ^{80,82,84}Sr isotopes have been performed. The Hamiltonian was

$$H=\epsilon(n_{d_\pi}+n_{d_\nu})+\kappa Q_\pi\cdot Q_\nu+aM\ ,$$

where

$$Q_\rho=(d^\dagger s+s^\dagger\tilde{d})_\rho+\chi_\rho(d^\dagger\tilde{d})_\rho,\quad \rho=\pi,\nu\ ,$$

$$M=\sum_{l=1,3}(d^\dagger_\pi\tilde{d}_\nu)^{(l)}\cdot(d^\dagger_\nu\tilde{d}_\pi)^{(l)}\ .$$

In the IBM, proton and neutron bosons are assumed to be in two states with angular momentum $L=0$ and 2 which are usually referred to as the boson s and d states. The total number of proton and neutron bosons are independently conserved. ϵ is the energy splitting between the s and d state. H is assumed to be equal for protons and neutrons. Hence the first part of the Hamiltonian describes the independent motion of the bosons which gives rise to a harmonic excitation spectrum. The operators $n_{d_{\pi,\nu}}$ are the proton and neutron d-boson number operators. The second and third terms of the Hamiltonian describe the proton-neutron interaction consisting of a quadrupole quadrupole and a Majorana-type exchange force. The parameters κ and a represent the strengths of these two types of forces. $Q_{\pi,\nu}$ is the proton- neutron-quadrupole operator. It is a linear combination of two terms, so that two additional parameters ($\chi_{\pi,\nu}$) determine the quadrupole force. The first two terms of the Hamiltonian resemble somehow the well known and widely used "pairing plus quadrupole" force. They determine essentially the structure of the IBM wave functions. The third term, the "Majorana force," is introduced more or less *ad hoc* to improve the position of unnatural parity levels. For ^{84}Sr the parameters ϵ,κ, were varied. χ_π was kept constant in all the Sr calculations while χ_ν was taken from Kr calculations.[17]

Figure 10 shows the comparison between experiment and theory for energies and Fig. 11 for

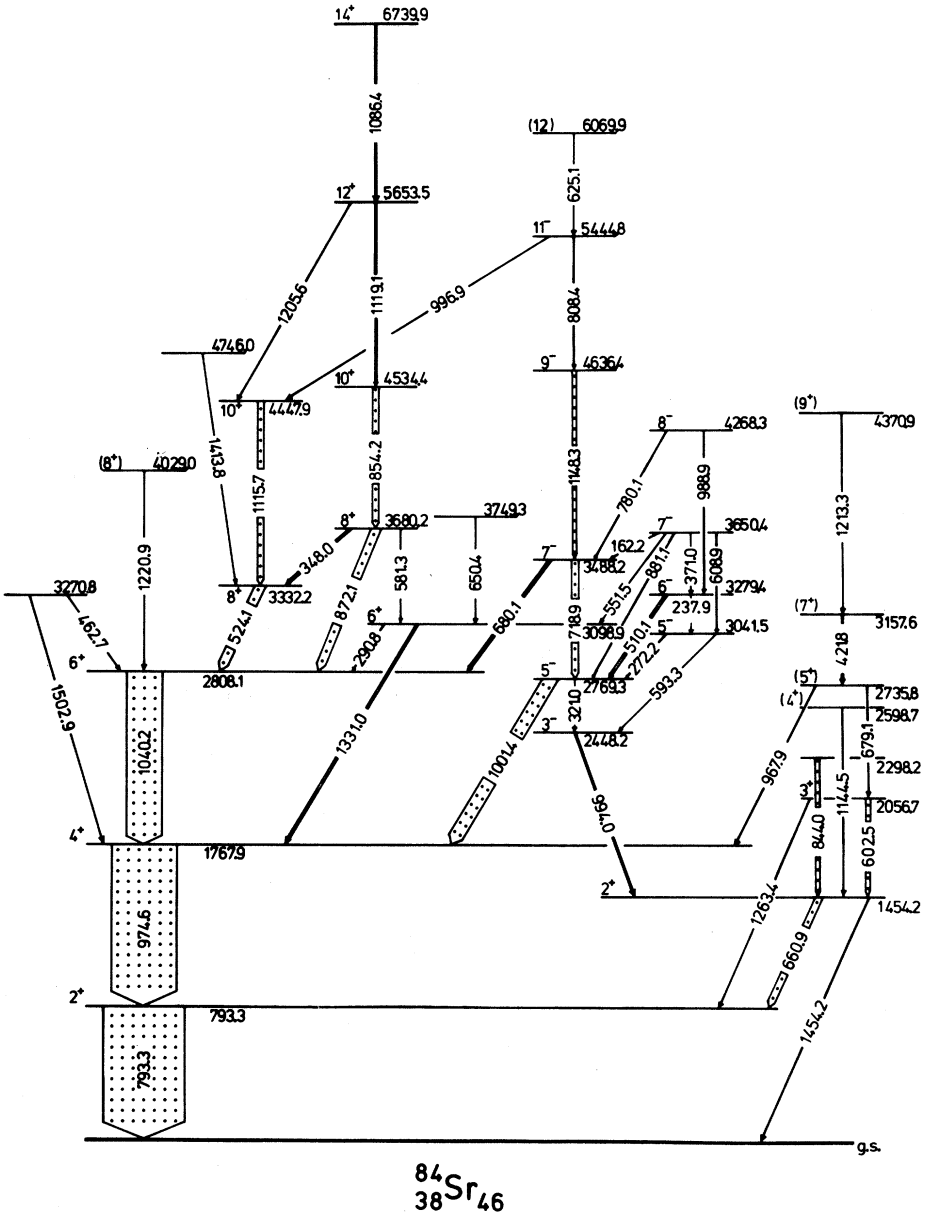

$^{84}_{38}Sr_{46}$

FIG. 8. Level scheme of ^{84}Sr showing transitions observed in the reactions ^{76}Ge(^{12}C,4n) and ^{81}Br(^{6}Li,3n). The widths of the arrows represent the relative intensities of the transitions found in the Li induced reaction.

$B(E2)$ values. While the calculated energies of the gsb and quasigamma band fit rather well, the experimental $B(E2)$ values are much lower than the theoretical ones. The deviations from the rotational values for the $4^+ \rightarrow 2^+$ and $6^+ \rightarrow 4^+$ transitions are even larger than those predicted by IBM due to the boson cutoff. This indicates that the states belonging to the gsb of ^{84}Sr are less collective than should be expected from the properties of both neighboring Kr isotopes ($A = 78, 80$) and lighter Sr isotopes.

A comparison shows that in ^{82}Sr the $B(E2)$'s are much larger and the energy pattern of the gsb is more rotational. A plausible explanation of the attenuation of the $B(E2)$ values in ^{84}Sr is the admixture of quasiparticle states setting in already at spin 4 in the gsb.

Besides the 0^+ and 2^+ states of the gsb and the 2^+ state of the quasi-γ band three additional 0^+ and 2^+ states have been observed using the (p,t) reaction.[6] The structure of these states is unidentified and therefore an association with states calcu-

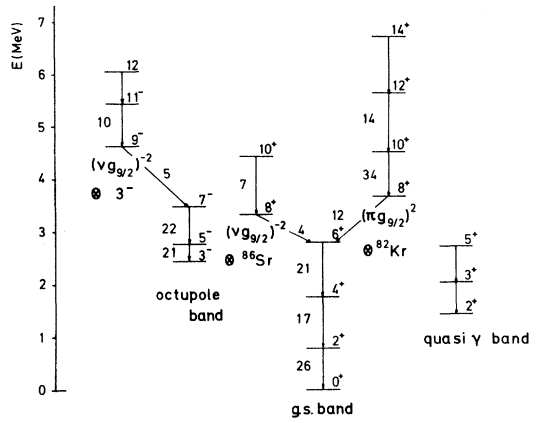

FIG. 9. Assumed band structure of ^{84}Sr; numbers left of the arrows indicate $B(E2)$ values in Weisskopf units (W.u.).

lated by the IBM is rather ambiguous. Due to that fact they have not been considered in the fit. Such states are predicted by the IBM calculation, but the agreement with experiment is poor with the exception of the 0_3^+ state.

The 8^+ state at 3332 keV is obviously a two quasiparticle excitation, as indicated by the $E2$ transition probability of 4.2 W.u. for the 524 keV transition, and can be interpreted as a two neutron hole $(\nu g_{9/2})_{8^+}{}^{-2}$ configuration coupled to the ^{86}Sr

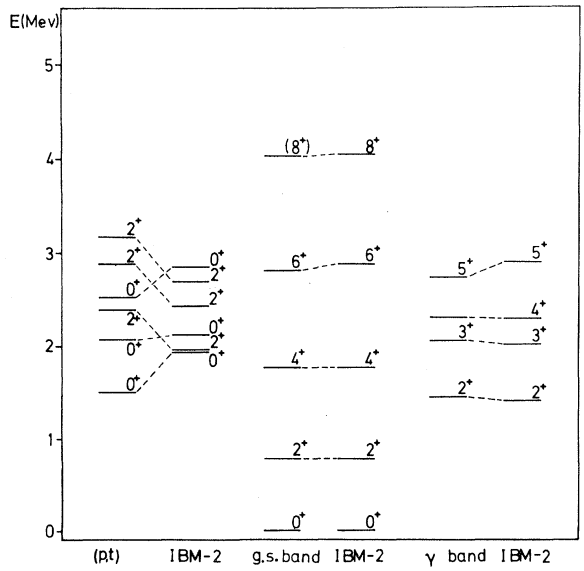

FIG. 10. Comparison of IBM fits with the experimental energies of the gsb, quasigamma band, and some states found in a (p,t) reaction (Ref. 6). Parameters: $\epsilon=1.14$; $\kappa=-0.145$; $\chi_\pi=-1,3$; $\chi_\nu=0.92$; and $a=0.1$.

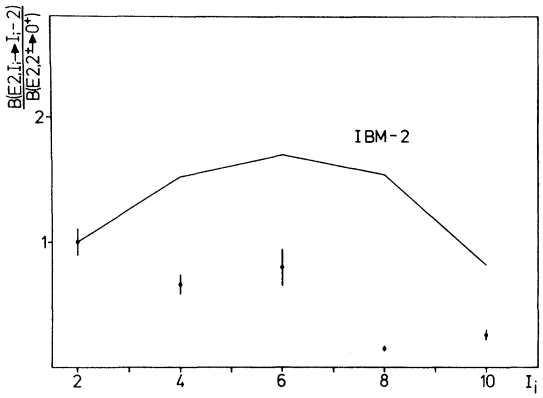

FIG. 11. Comparison between experimental and theoretical $E2$ transition strengths. The $B(E2)$'s are normalized to the $B(E2,2^+\rightarrow 0^+)$ value.

ground state. Such $(\nu g_{9/2})_{8^+}{}^{-2}$ states have been found in most $N=46$ and $N=48$ isotopes. The neutron origin of this state in ^{84}Sr could be established definitely only by means of a g-factor measurement. Since a value of $B(E2;\ 10^+\rightarrow 8^+)=6.8$ W.u. is also rather small, we interpret the 4448 keV 10^+ state as being the same $(\nu g_{9/2})_{8^+}{}^{-2}$ state coupled to the 2_1^+ of the ^{86}Sr core. The energy difference $E_{10^+\rightarrow 8^+}=1116$ keV is very close to the corresponding energy interval $E_{2^+\rightarrow 0^+}=1077$ keV in ^{86}Sr.

The second 8^+ state at 3680 keV cannot belong to the gsb or to the quasigamma band because of its low energy and relatively small value of $B(E2,8_2^+\rightarrow 6^+)=12$ W.u. We shall tentatively assume that we deal with a two proton $(\pi g_{9/2})_{8^+}{}^{2}$ state coupled to a ^{82}Kr core; the energy of the $10^+\rightarrow 8^+$ transition is 854 keV, which is not far from $E_{2^+\rightarrow 0^+}=776$ keV in ^{82} Kr.

Turning our attention now to negative parity states, we notice the presence of a 3^- state whose spin parity assignment is unambiguous.[6] We consider this state having an octupole nature; it is probably made out of particle-hole excitations such as $(g_{9/2},f_{5/2}{}^{-1})$, $(g_{9/2},p_{3/2}{}^{-1})$, etc. The $5^-\rightarrow 3^-$ transition has collective strength, therefore we can assume that a collective band is built upon the 3^- state. The $B(E2;9^-\rightarrow 7^-)$ value of 5.2 W.u. indicates that the 9^- 4636 keV state has a different intrinsic structure. We can interpret it as having a $3^-\otimes(\nu g_{9/2})^{-2}$ configuration.

IV. CONCLUSION

The main feature of ^{84}Sr is the interplay of collective and independent particle excitations. The

distinction between these two excitation modes was made by means of measured reduced $E2$ transition probabilities.

The energies of collective states were described in a satisfactory way by the interacting boson model. Deviations of experimental $B(E2)$ values from theoretical ones were attributed to the mixing of two quasiparticle states. A $(\nu g_{9/2})^{-2}$ configuration has been attributed to the first 8^+ excited state; this configuration has been observed in most $N=48$ isotones.

ACKNOWLEGDMENTS

We would like to thank Mr. K. Neuenhofer for his help in analyzing the data and Dr. D. Bazzacco for useful discussions. We thank Mr. H. Bohnhoff and his crew at the Cologne FN tandem for their cooperation. This work was supported by the German BMFT.

[1]I. Talmi and I. Unna, Nucl. Phys. 19, 225 (1960).
[2]N. Auerbach and I. Talmi, Nucl. Phys. 64, 458 (1965).
[3]J. E. Kitching *et al.*, Nucl. Phys. A177, 433 (1971).
[4]K. Ogawa, Phys. Lett. 45B, 214 (1973).
[5]H.-W. Müller and J. W. Tepel, Nucl. Data Sheets 27, 339 (1979).
[6]J. B. Ball, J. J. Pinajian, J. S. Larsen, and A. C. Rester, Phys. Rev. C 8, 1438 (1973).
[7]D. C. Montague, K. Ramavataram, and N. S. Chant, W. G. Davies, J. E. Kitching, W. McLatchie, and J. M. Morton, Z. Phys. 261, 155 (1973).
[8]A. C. Rester, B. van Nooijen, P. Spilling, J. Konijn, and J. J. Pinajian, Phys. Rev. C 7, 210 (1973).
[9]T. Inamura, S. Nagamiya, A. Hashizume, and Y. Tendow, Institute of Physical and Chemical Research, Japan, Cyclotron Progress Report No. 5, 1971 (unpublished), p. 46.
[10]N. Yoshikawa, Y. Shida, O. Hashimoto, M. Sakai, and T. Numao, Nucl. Phys. A327, 477 (1979).
[11]K. P. Lieb, M. Uhrmacher, J. Dauk, and A. M. Kleinfeld, Nucl Phys. A223, 445 (1974).
[12]T. K. Alexander and A. Bell, Nucl. Instrum. Methods 81, 22 (1970).
[13]R. Rascher, K. P. Lieb, and M. Uhrmacher, Phys. Rev. C 13, 1217 (1976).
[14]H. P. Hellmeister, University of Köln, 1976 (unpublished).
[15]H. P. Hellmeister, K. P. Lieb, and W. Müller, Nucl. Phys. A307 515 (1978).
[16]T. Otsuka, A. Arima, F. Iachello, and I. Talmi, Phys. Lett. 76B, 139 (1978).
[17]U. Kaup and A. Gelberg, Z. Phys. A 293, 311 (1979).